

# Integrated Sachs-Wolfe effect in Cross-Correlation: The Observer's Manual

Niayesh Afshordi\*

*Princeton University Observatory, Princeton University, Princeton, NJ 08544*

The Integrated Sachs-Wolfe (ISW) effect is a direct signature of the presence of dark energy in the universe, in the absence of spatial curvature. A powerful method for observing the ISW effect is through cross-correlation of the Cosmic Microwave Background (CMB) with a tracer of the matter in the low redshift universe. In this paper, we describe the dependence of the obtained cross-correlation signal on the geometry and other properties of a survey of the low redshift universe. We show that an all-sky survey with about 10 million galaxies, almost uniformly distributed within  $0 < z < 1$  should yield a near optimal ISW detection, at  $\sim 5\sigma$  level. In order to achieve this level of signal-to-noise, the systematic anisotropies in the survey must be below  $\sim 0.1\%$ , on the scale of  $\sim 10$  degrees on the sky, while the systematic error in redshift estimates must be less than 0.05.

Then, we argue that, while an ISW detection will not be a good way of constraining the conventional properties of dark energy, it could be a valuable means of testing alternative theories of gravity on large physical scales.

PACS numbers: 98.65.Dx, 98.62.Py, 98.70.Vc, 98.80.Es

## I. INTRODUCTION

One of the fundamental pieces of our understanding of modern cosmology comes from the study of anisotropies in the Cosmic Microwave Background (CMB). First discovered by the DMR experiment on the COBE satellite in the early 90's [1], the observations of CMB anisotropies matured through various ground-based/balloon-borne experiments (see [2] for a list) until its latest climax by the first year data release of the observations of the WMAP satellite [2] in 2003, a cosmic variance limited map of the CMB sky with a resolution of  $\lesssim 0.5$  degs.

While most of the fluctuations seen by WMAP and other CMB experiments were generated at  $z \sim 1000$ , low redshift ( $z < 20$ ) physics generates additional fluctuations [3]. These secondary anisotropies can be detected through cross-correlating CMB measurements with large scale structure observations [4, 5]. Following the WMAP data release, various groups [6] claimed a possible observation of such correlation with various galaxy surveys, although at a small ( $2 - 3\sigma$ ) significance level. Most recently, [7] claimed a correlation between WMAP maps and the 2MASS galaxy catalog, at both large and small angles.

In this paper, we focus on such correlations on angles larger than a few degrees, and their only known cosmological source, the Integrated Sachs-Wolfe (ISW) effect [8]. The purpose of this work is to provide comprehensive overview of various observational aspects and systematic limitations of an ISW detection in cross-correlation, in a flat universe. Secs. II and III will briefly review the physics of the expected signal and error in any ISW de-

tection. In Sec. IV, we consider over what redshift range, and what angular scales, most of the ISW signal arises, and what the optimum signal-to-noise for an ISW detection may be. Sec. V deals with the limitations of realistic surveys, i.e. the Poisson noise, systematic contaminations, and redshift errors. Finally, in Sec. VI, we discuss what we may (or may not) learn from a detection of the ISW signal in cross-correlation, and Sec. VII concludes the paper.

Throughout this paper, unless mentioned otherwise, we use the flat 1st year WMAP+CBI+ACBAR+2dF+Ly- $\alpha$  concordance cosmological model ( $\Omega_m = 0.27$ ,  $\Omega_\Lambda = 0.73$ , and  $\sigma_8 = 0.84$  [9]), with a cosmological constant (i.e.  $w = -1$ ), and a running spectral index ( $n_s = 0.93$ , and  $dn_s/d\ln k = -0.031$  at  $k = 0.05 h/\text{Mpc}$ ). However, note that our conclusions are not sensitive to the details of the model.

In this paper, the 3D Fourier transform is defined as

$$A_{\mathbf{k}} = \int d^3\mathbf{x} A(\mathbf{x}) \exp(-i\mathbf{k}\cdot\mathbf{x}), \quad (1)$$

while the cross-power spectrum of fields  $A$  and  $B$ ,  $P_{A,B}$ , is defined through

$$\text{Re}\langle A_{\mathbf{k}} B_{\mathbf{k}'}^* \rangle = (2\pi)^3 \delta_{\mathbf{D}}^3(\mathbf{k} - \mathbf{k}') P_{A,B}(k), \quad (2)$$

where  $\delta_{\mathbf{D}}^3$  is the 3D Dirac delta function. The auto-power spectrum is also defined in a similar way.

## II. THE ISW EFFECT IN CROSS-CORRELATION

The ISW effect is caused by the time variation in the cosmic gravitational potential,  $\Phi$ , as CMB photons pass through it. In a flat universe, the anisotropy in CMB

---

\*Electronic address: afshordi@astro.princeton.edu

photon temperature due to the ISW effect[8] is an integral over the conformal time  $\eta$

$$\delta_{\text{ISW}}(\hat{\mathbf{n}}) = \frac{\delta T_{\text{ISW}}}{T} = 2 \int_{\eta_{\text{LS}}}^{\eta_0} \Phi'[(\eta_0 - \eta)\hat{\mathbf{n}}, \eta] d\eta, \quad (3)$$

where  $\Phi' \equiv \partial\Phi/\partial\eta$ , and  $\hat{\mathbf{n}}$  is the unit vector along the line of sight.  $\eta_{\text{LS}}$  and  $\eta_0$  are the conformal times at the last scattering and today, while the speed of light is set equal to unity ( $c = 1$ ). The linear metric is assumed to be

$$ds^2 = a^2(\eta) \{ [1 + 2\Phi(\mathbf{x}, \eta)] d\eta^2 - [1 - 2\Phi(\mathbf{x}, \eta)] d\mathbf{x} \cdot d\mathbf{x} \}, \quad (4)$$

(the so-called longitudinal gauge) and  $\eta_0$  is the conformal time at the present.

In a flat universe, in the linear regime,  $\Phi$  does not change with time at any given comoving point for a fixed equation of state [30], and therefore observation of an ISW effect is an indicator of a change in the equation of state of the universe. Assuming that this change is due to an extra component in the matter content of the universe, the so-called dark energy, this component should have a negative pressure to become important at late times [10]. Therefore, observation of an ISW effect in a flat universe is a signature of dark energy.

The ISW effect is observed at large angular scales because most of the power in the fluctuations of  $\Phi$  is at large scales. Additionally, the fluctuations at small angles tend to cancel out due to the integration over the line of sight.

We are interested in finding the cross-correlation of the ISW effect with the galaxy distribution. Assuming Gaussian initial conditions, and full-sky coverage, different harmonic multipoles are statistically independent in the linear regime. Therefore, as the ISW effect is only important on large scales which are still linear, the statistical analysis is significantly simplified in harmonic space. For a galaxy survey with the average comoving density distribution  $n_c(r)$  as a function of the comoving distance  $r$ , the Limber equation can be used to approximately describe the expected cross-correlation with the galaxy distribution [31] (see [7] for detailed derivation)

$$C_{gT}(\ell) \equiv \langle \delta_{g,\ell m}^{2D} T_{\ell m}^* \rangle = \frac{2T}{\int dr r^2 n_c(r)} \int dr n_c(r) P_{\Phi',g} \left( \frac{\ell + 1/2}{r} \right), \quad (5)$$

where  $\delta_{g,\ell m}^{2D}$  and  $T_{\ell m}$  are the projected survey galaxy overdensity and the CMB temperature in the spherical harmonic space. If we assume that the galaxies follow the matter density with constant bias,  $b_g$ , (i.e.  $\delta_g = b_g \delta_m$ ), then  $P_{\Phi',g}(k)$ , the 3D cross-power spectrum of  $\Phi'$  and galaxy overdensity for the comoving wave-number  $k$ , can be related directly to  $P_{\Phi',m}$ . We then use the  $G_{00}$  Einstein equation [11]

$$(k^2 + 3\mathcal{H}^2)\Phi + 3\mathcal{H}\Phi' + 4\pi G a^2 (\rho_m \delta_m + \rho_{DE} \delta_{DE}) = 0, \quad (6)$$

to relate the matter auto-power spectrum  $P_{m,m}(k) = P(k)$  to  $P_{\Phi',g}$ . Here,  $\mathcal{H} = d \ln a / d\eta$  is the conformal Hubble

constant, and  $\rho_{DE}$  and  $\delta_{DE}$  are the average density and overdensity of the dark energy, respectively.

Note that, for a cosmological constant (a  $\Lambda$ CDM cosmology),  $\delta_{DE} = 0$ , and Eq. (6) reduces to the Poisson equation for  $k \gg \mathcal{H}$ . In this case, Eq. (5) reduces to

$$C_{gT}(\ell) = - \frac{3b_g H_0^2 \Omega_m}{\int dr r^2 n_c(r)} \times \int dr r^2 n_c(r) \cdot \frac{1+z}{(\ell + 1/2)^2} \cdot \frac{g'}{g} P \left( \frac{\ell + 1/2}{r} \right), \quad (7)$$

where  $g$  is the linear growth factor of the gravitational potential,  $\Phi$ , and  $g'$  is its derivative with respect to the conformal time, while  $z$  denotes the cosmological redshift, which is related to the comoving distance  $r$  via

$$\frac{dz}{1+z} = \mathcal{H} dr. \quad (8)$$

For any alternative theory of dark energy, an independent equation for the evolution of  $\delta_{DE}$  should be solved simultaneously.

### III. THE ERROR IN ISW DETECTION

It is easy to see that the expected dispersion (see [7] for details [32]) in the cross-correlation signal for harmonic multipole  $C_{gT}(\ell)$  is given by

$$\Delta C_{gT}^2(\ell) \simeq \frac{C_{gg}(\ell) C_{TT}(\ell)}{f_{\text{sky}} (2\ell + 1)}, \quad (9)$$

where  $f_{\text{sky}}$  is the fraction of sky covered in the survey, and we assumed a small cross-correlation signal, i.e.  $C_{gT}^2(\ell) \ll C_{gg}(\ell) C_{TT}(\ell)$ , which is the case for the ISW effect (the expected ISW effect is much smaller than the primary anisotropies, but see [12]).

$C_{TT}(\ell)$  is the observed CMB temperature auto-power, which includes both the intrinsic CMB fluctuations and the detector noise. As will become clear later on, since the ISW effect is observed at small  $\ell$ , the WMAP observed auto-power spectrum [13], which has negligible detector noise at low  $\ell$ , should give the optimum power spectrum to use in Eq. (9). We again use the Limber approximation to obtain the projected galaxy auto-power

$$C_{gg}(\ell) \simeq \frac{\int dr r^2 n_c^2(r) [b_g^2(r) \cdot P \left( \frac{\ell + 1/2}{r} \right) + n_c^{-1}(r)]}{[\int dr r^2 n_c(r)]^2}. \quad (10)$$

Fig. (1) shows an example of the expected cross-power signal and error for a survey with 10 million galaxies with  $b_g = 1$ , uniformly distributed between  $0 < z < 1$ .

### IV. THE PERFECT GALAXY SURVEY

To obtain the optimum signal-to-noise ratio for an ISW detection in cross-correlation, we assume that we have an

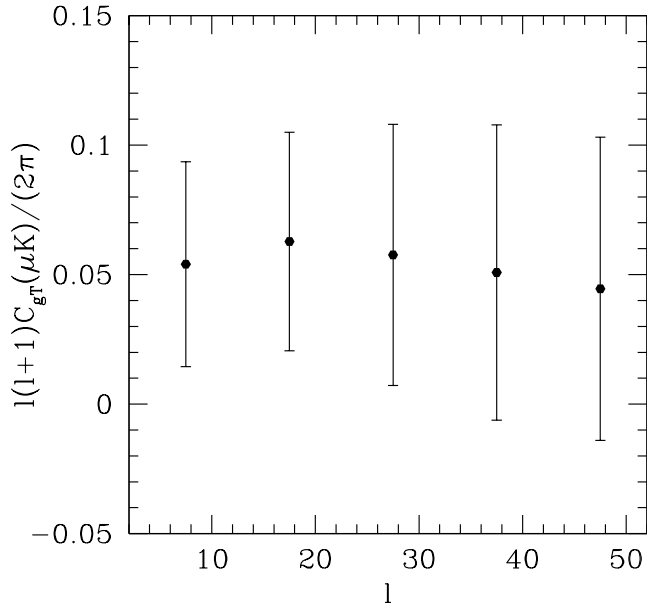


FIG. 1: The expected cross-power spectrum of the ISW effect, for an all-sky survey with  $b_g^2 dN/dz = 10^7$ , and  $z_{\max} = 1$

(at least approximate) redshift estimate for each galaxy in the survey. Then we can divide the survey into almost independent shells of thickness  $\delta r$ , where

$$r_0 \ll \delta r \ll r,$$

where  $r_0 \lesssim 5h^{-1}\text{Mpc}$  is the galaxy auto-correlation length. Using Eq. (5), the expected ISW cross-power signal for a narrow redshift bin  $(z, z + \delta z)$ , at multipole  $\ell$ , is

$$C_{gT}(\ell, z) = \frac{2b_g(r)}{r^2(z)} P_{\Phi', m} \left( \frac{\ell + 1/2}{r} \right), \quad (11)$$

while Eq.(9) gives the error in the cross-power spectrum

$$\Delta C_{gT}^2(\ell, z) = \frac{C_{TT}(\ell) C_{gg}(\ell, z)}{2\ell + 1}, \quad (12)$$

and Eq.(10) can be used to find  $C_{gg}(\ell, z)$

$$C_{gg}(\ell, z) = \frac{b_g^2(r)}{r^2 \delta r} \left[ P \left( \frac{\ell + 1/2}{r} \right) + (n_c b_g^2)^{-1} \right]. \quad (13)$$

Dividing Eq. (11) by Eq. (12), we find the expected signal-to-noise ratio for the cross-correlation signal in multipole  $\ell$ , due to this shell

$$\delta(S/N)^2 = \frac{C_{gT}^2(\ell)}{\Delta C_{gT}^2(\ell)} = \frac{[r^{-2} \delta r \cdot (2\ell + 1)] \times 4P_{\Phi', m}^2(k)}{C_{TT}(\ell) [P(k) + (n_c b_g^2)^{-1}]}, \quad (14)$$

where  $k = \frac{\ell+1/2}{r}$ . Within the approximation of independent shells and multipoles,  $(S/N)^2$  is cumulative, and we

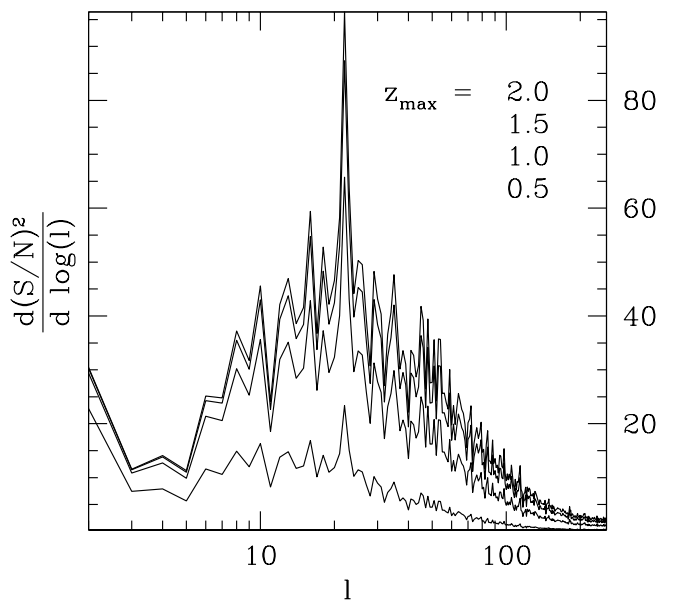
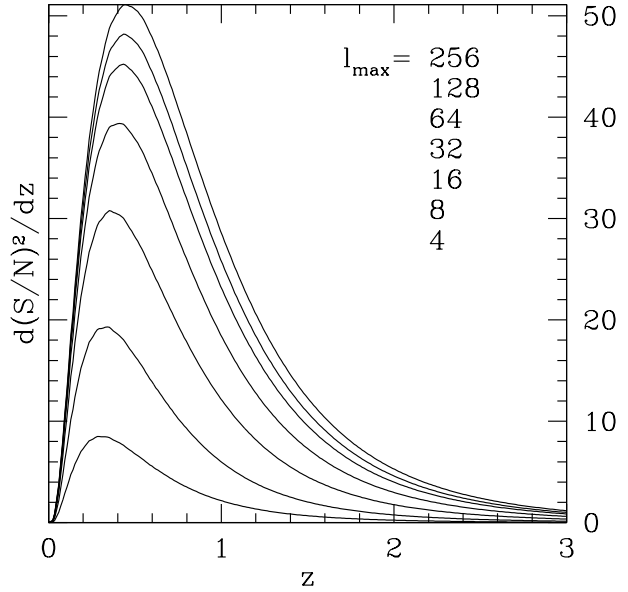


FIG. 2: Figures show the expected  $(S/N)^2$  distribution for a redshift or resolution limited full-sky ISW cross-correlation signal ( $\ell_{\max}$  refers to the scale at which the (white) detector noise is equal to the true signal). In either figures, the enclosed area for the region covered by a survey, multiplied by its sky coverage, gives the optimum  $(S/N)^2$  for the cross-correlation signal. The spikiness of the distribution in  $\ell$ -space is due to the use of the actual observed WMAP power spectrum in Eq. (14). Note that for partial sky coverage, the low- $\ell$  multipoles that are not covered by the survey should also be excluded from the area under the curves.

could simply add (or integrate over) the contribution due to different multipoles and shells that are included in the galaxy survey, and multiply it by the sky coverage,  $f_{\text{sky}}$ , to obtain the optimum  $(S/N)^2$  (in the absence of systematics) for the whole survey. Fig. (2) shows the  $(S/N)^2$  density distribution for hypothetical all-sky surveys with limited (CMB) resolution, or redshift depth, in a  $\Lambda$ CDM cosmology, while we assumed that the Poisson noise is negligible ( $n_c \rightarrow \infty$ ).

We see that the ISW cross-correlation signal is widely distributed over a redshift range between 0 and 1.5 (which is the era in which dark energy becomes cosmologically important), and peaks at  $z \simeq 0.4$ , below which the detection is limited by the available volume. Almost all the signal is due to multipoles with  $\ell \lesssim 100$  ( $\theta \gtrsim 2^\circ$ ), which implies that the WMAP 1st year all-sky temperature map [2], with  $S/N \gg 1$  on scales larger than a degree ( $\ell < 200$ ), captures almost all the ISW signal in the CMB sky, while the upcoming 2nd year WMAP data, or higher resolution CMB observations are unlikely to make a significant difference. The angular scale of the cross-correlation signal decreases with the depth of the survey. This is due to the fact that the angular correlation length of the galaxy distribution is smaller for a deeper (more distant) sample.

For our assumed  $\Lambda$ CDM cosmological model, the total  $S/N$  which could be achieved by a perfect survey is  $\sim 7.5$ . Let us compare this result with previous such estimates. The first estimate of  $S/N$  for a perfect survey [4] is, in fact, completely consistent with  $7.5\sigma$ . Other such estimates [5] focus on specific surveys, but seem to be roughly consistent with the values expected from Fig. (2) for those surveys. This is despite our use of Limber (Eq. 5) and independent redshift bins (Eq. 19) approximations, and demonstrates that these approximations are adequate for our purpose. Our approach allows us to visualize where in redshift-angular space one should look for the ISW signal. However, given a sample of galaxies in existence, we should emphasize that neither we, nor previous works, provide an optimum procedure to estimate this signal. For a realistic galaxy survey, such procedure would depend on possible survey contaminations or systematics, detailed geometry, and redshift information available for the survey (See the next section).

## V. SUB-OPTIMAL GALAXY SURVEYS

In this section we look into how different features of realistic surveys may reduce the optimum ISW signal-to-noise obtained in the last section.

### A. Poisson Limited Surveys

For a realistic survey, an additional source of noise is Poisson fluctuations in the galaxy number density. The Poisson noise (the second term in the brackets in Eq. 10)

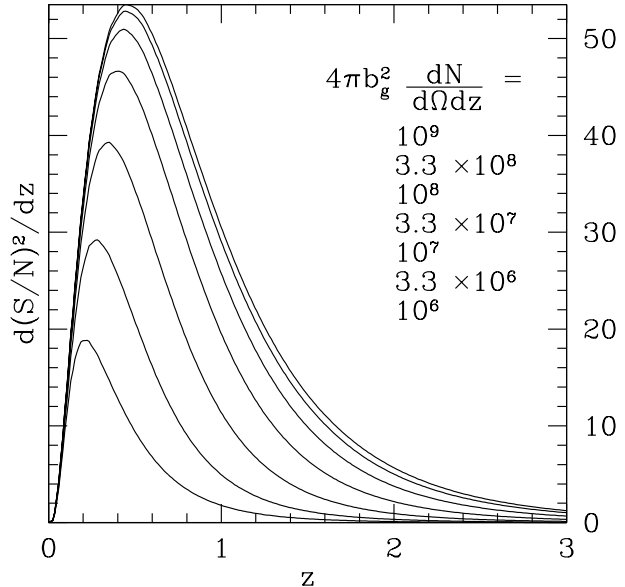


FIG. 3: The distribution of  $(S/N)^2$  for different galaxy redshift distributions. For partial sky coverage, the result should be multiplied by  $f_{\text{sky}}$ .

is inversely proportional to the average number density of observed galaxies in the survey, which dominates the uncertainty in cross-correlation for a small galaxy sample.

Figs. (3-4) show how the total cross-correlation  $(S/N)^2$  and its distribution depend on the number of galaxies in an all-sky survey. Although a fixed number of galaxies per unit redshift is assumed, different curves in Fig. (3) can be combined to obtain the signal-to-noise for an arbitrary redshift/bias distribution.

Fig. (4) shows that an ambitious all-sky survey with about 10 million galaxies (or one million clusters with  $b_g \sim 3$ ), which uniformly cover the redshift range between 0 to 1, can only yield a  $S/N$  of  $\simeq 5$ . Although the Sloan Digital Sky Survey (SDSS; [14]) is unlikely to get a  $S/N$  better than  $4\sigma$  due to its incomplete redshift and sky coverage, future galaxy surveys like LSST and Pan-STARRS could achieve a cosmic variance limited detection of ISW in cross-correlation [15], should they cover almost all of sky, and have sufficiently small systematic errors (see Sec. VB).

### B. Observational Contamination

Another feature of a realistic galaxy survey is the presence of artificial structure in the sky maps. Such structures may be due to observational systematics, such as day to day changes of weather, seeing or photometric calibrations. Another possibility is the effective change of magnitude limit due to Galactic extinction, or Galactic

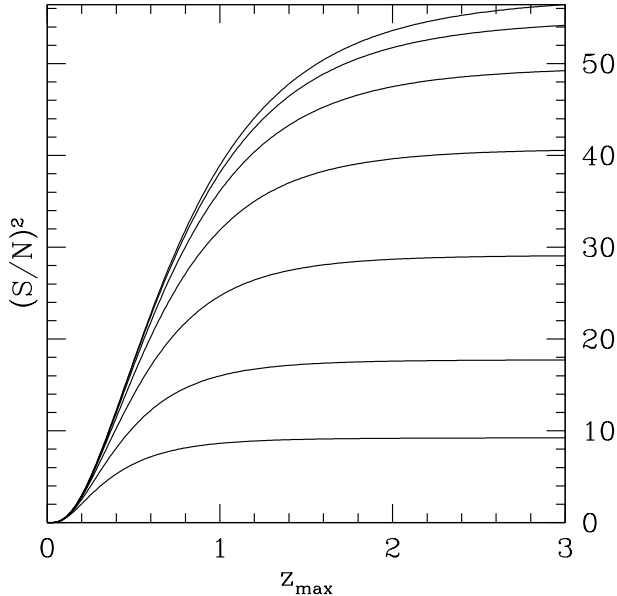


FIG. 4: The integrated (total)  $(S/N)^2$  for a constant  $dN/dz$  up to  $z_{\max}$ , corresponding to the area under the curves in Fig. 3.

contamination due to stars misidentified as galaxies. Depending on if these contaminations are correlated with possible contaminations of the CMB maps, they can add extra random or systematic errors to the optimum error that may be achieved by a survey.

### 1. Uncorrelated Contaminations: Random Errors

If the contaminations of the galaxy survey is not correlated with the contaminations in the CMB map, they should not affect the expectation value of the cross-correlation function of the galaxy survey with the CMB. We do not expect the observational systematics of the galaxy/CMB surveys to be correlated. Therefore, the only effect will be to increase the random error through increasing the auto-powers of each survey (Eq. 9). Since the Galactic/systematic contributions to the power spectrum of the CMB are believed to be small and under control [13, 16], we focus on the contamination of the galaxy survey.

We again divide our galaxy sample into independent redshift bins. The harmonic components of the anisotropies in each redshift bin can be divided into real and systematic parts:

$$\tilde{\delta}_g(\ell, m; z) = \delta_g(\ell, m; z) + \delta_g^{sys}(\ell, m). \quad (15)$$

While the systematic contaminations,  $\delta_g^{sys}(\ell, m)$ , is also, in general, a function of redshift, for simplicity, we ignore this dependence. Of course, in practice, the level of systematics in the redshift range that contains the bulk of

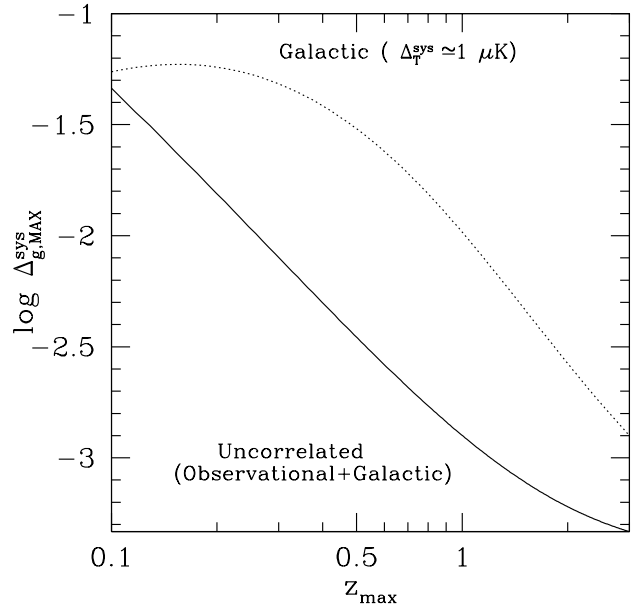


FIG. 5: The graph shows the maximum allowed amplitude of anisotropies,  $\Delta_g^{sys}$  introduced by possible systematics of the galaxy survey. The solid line shows the level of systematics that reduces the  $(S/N)^2$  for an ISW detection by 50%. The dotted line shows the level of *correlated* contamination that introduces a systematic error in an ISW detection comparable to the cosmic variance. Here, we assume that the correlated amplitude of CMB contamination is  $\sim 1\mu K$ , consistent with the expected leftover Galactic contamination in WMAP foreground-cleaned W-band map [16].

the ISW signal is the relevant quantity (see Figs. 2-3). Now, the contaminated auto-power spectrum will be

$$\tilde{C}_{gg}(\ell; z_1, z_2) = C_{gg}(\ell; z_1)\delta_{z_1, z_2} + C_{gg}^{sys}(\ell), \quad (16)$$

where  $C_{gg}(\ell, z)$  was defined in Eq. (13), and we ignore the cross-term, as we do not expect any correlation between the survey systematics and the intrinsic fluctuations in the galaxy density. Note that, unlike the previous sections, different redshift bins are now correlated, and we will need to invert the full covariance matrix to estimate the expected signal to noise. Eq. (9) can be generalized to get the covariance matrix of the cross-power spectrum for  $f_{sky} = 1$

$$\begin{aligned} \tilde{C}_{\ell; z_1, z_2} &= \langle \Delta C_{gT}(\ell, z_1) \Delta C_{gT}(\ell, z_2) \rangle \\ &= \frac{\tilde{C}_{gg}(\ell; z_1, z_2) C_{TT}(\ell)}{2\ell + 1}. \end{aligned} \quad (17)$$

For a low level of systematics, we can use a Taylor expansion to invert the covariance matrix

$$\tilde{C}^{-1} \simeq C^{-1} - C^{-1} C^{sys} C^{-1}. \quad (18)$$

Now combining Eqs. (11,12, and 16-18) yields an approximate expression for the suppression of  $(S/N)^2$  due

to the presence of contaminations:

$$\begin{aligned} \delta(S/N)^2 &\simeq - \sum_{z_1, z_2, \ell} (2\ell + 1) \frac{C_{gg}^{sys}(\ell) C_{gT}(\ell, z_1) C_{gT}(\ell, z_2)}{C_{TT}(\ell) C_{gg}(\ell, z_1) C_{gg}(\ell, z_2)} \\ &= - \sum_{\ell} (2\ell + 1) \frac{C_{gg}^{sys}(\ell)}{C_{TT}(\ell)} \left( \sum_z \frac{C_{gT}(\ell, z)}{C_{gg}(\ell, z)} \right)^2. \end{aligned} \quad (19)$$

Let us define the amplitude of the systematic contaminations,  $\Delta_g^{sys}$  as

$$\Delta_g^{sys} \equiv \sqrt{\frac{\ell(\ell + 1) C_{gg}^{sys}(\ell)}{2\pi}}. \quad (20)$$

Again, for simplicity, we assume that  $\Delta_g^{sys}$  is independent of  $\ell$ . Of course, the relevant amplitude for  $\Delta_g^{sys}$  corresponds to the  $\ell$ -range that contains the bulk of the ISW signal, i.e.  $\ell \sim 20$  (see Fig. 2). The solid line in Fig. (5) shows the amplitude of uncorrelated contamination, required to reduce the  $(S/N)^2$  by 50%. Thus, we see that since we need  $z_{max} \gtrsim 1$  to capture most of the ISW signal (see Sec. IV), the level of systematic anisotropy in the galaxy survey should be less than 0.1% on scales of  $\ell \sim 20$ .

As an example, let us assume the systematic anisotropy in an optical survey is due to uncertainties in the magnitude calibration. Furthermore, let us assume that we know the (approximate) redshifts, and in a given redshift bin, the luminosity function is given by the Schechter function [20]:

$$\phi(L) dL = \phi^* \cdot (L/L^*)^\alpha \exp(-L/L^*) (dL/L^*) \quad (21)$$

where  $\phi^*$ ,  $L^*$ , and  $\alpha$  are characteristic galaxy number density, luminosity, and slope of the luminosity function, respectively. Assuming that the survey is almost complete in the given redshift bin, i.e.  $L_{min} \ll L^*$ , the systematic anisotropy is given by:

$$\Delta_g^{sys} = \frac{\phi(L) \Delta L_{min}}{\int \phi(L) dL} = (L_{min}/L^*)^{1+\alpha} \frac{\Delta L_{min}/L_{min}}{\Gamma(1+\alpha)}. \quad (22)$$

For  $\alpha \simeq -0.9$  [17], we can ignore  $1 + \alpha$  in the exponent, and use  $\Delta L/L = 0.4 \ln(10) \Delta m$ , to arrive at

$$\Delta_g^{sys} \simeq \frac{0.4 \ln 10 \Delta m}{\Gamma(1+\alpha)} \simeq 0.1 \Delta m < 10^{-3}, \quad (23)$$

where  $\Delta m$  is the uncertainty in the magnitude calibration. Thus, we see that  $\Delta m$  needs to be  $\lesssim 0.01$ , for the error to be dominated by cosmic variance. The accuracy of this calibration is currently  $\sim 0.02$  for SDSS [18], and will remain a challenge for future surveys such as Pan-STARRS and LSST. Note that the magnitude uncertainty of individual galaxies, as long as they are not correlated on the scale of a few degrees on the sky, can be significantly larger.

Repeating this estimate for an incomplete survey. i.e.  $L_{min} > L^*$ , we see that a significantly higher precision of

magnitude measurement will be required to capture the ISW signal:

$$\Delta m \lesssim \begin{cases} 0.01 & \text{for } L_{min} \ll L^*, \\ 10^{-3} \frac{L^*}{L_{min}} & \text{for } L_{min} \gg L^*. \end{cases} \quad (24)$$

## 2. Galactic Contaminations: Systematic Errors

As the Galactic sources of contamination in the CMB and galaxy surveys are correlated, they may cause a systematic over/underestimate of the cross-correlation signal. In order to model this effect, we assume that this correlated signal follows the Schlegel, Finkbeiner, and Davis (SFD) Galactic extinction map [19]. Since the bulk of the ISW signal comes from  $\ell \sim 20$ , we normalize the amplitude of the contaminating signals at  $\ell = 20$ . The level of Galactic contamination in the foreground cleaned W-band of the WMAP satellite [16] is expected to be  $\sim 1 \mu K$  outside the Galactic plane, and thus we take

$$\Delta_T^{sys}(\ell) \equiv \sqrt{\frac{\ell(\ell + 1) C_{gg}^{sys}(\ell)}{2\pi}} = 1 \mu K, \quad \text{for } \ell = 20, \quad (25)$$

while we assume  $C_{gg}^{sys} \propto C_{TT}^{sys} \propto C_{SFD}$ , for the  $\ell$ -dependence of the correlated contamination. Here,  $C_{SFD}$  is the angular auto-power spectrum of the SFD extinction map.

The dotted line in Fig. (5) shows the amplitude of the correlated systematic anisotropy, normalized at  $\ell = 20$ , which yields a systematic error in the ISW signal equal to the cosmic variance error. Since this systematic error is proportional to  $\Delta_T^{sys} \times \Delta_g^{sys}$ , the upper bound,  $\Delta_{g,MAX}^{sys}$ , shown in this figure decreases for larger Galactic contaminations in the CMB, inversely proportional to  $\Delta_T^{sys}$ . Thus, we see that since the solid curve is below the dotted curve, as long as  $\Delta_T^{sys} < \text{few } \mu K$ , the level of uncorrelated contamination puts a more stringent constraint on the systematics of the galaxy survey. As we discussed in Sec. VB 1, this requires the systematic anisotropy of the survey to be less than 0.1 %.

## C. Redshift errors

Since the ISW kernel has such a broad distribution in redshift space, redshift errors are not expected to be a big limiting factor for ISW cross-correlation measurements.

We can simulate *random* errors in the estimated redshifts, via re-writing Eq. (19) for finite redshift bins of thickness  $2\Delta z$ . It turns out that even using bins as thick as  $\Delta z \sim 0.5$  will not decrease the signal-to-noise by more than 5%.

*Systematic* errors in redshifts, or in redshift distribution, may also systematically bias the estimates of ISW amplitude. Taking the unbiased ISW amplitude to be

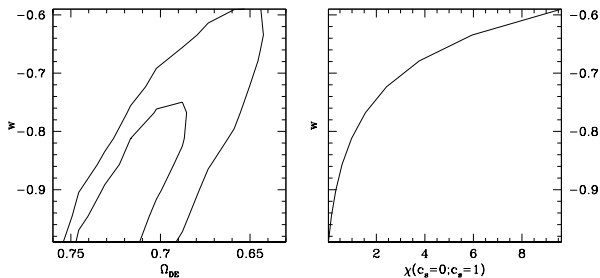


FIG. 6: (Left) The  $w - \Omega_m$  constraints (68% and 95% contours) based on an optimum ISW detection. (Right) The significance of ruling out  $c_s = 0$ , for a quintessence model with given  $w$ , and  $c_s = 1$ , based on an optimum ISW detection. In both graphs, other cosmological parameters are kept constant.

one, the ISW amplitude, biased by the systematic redshift error  $\Delta z$  is given by

$$1 + \frac{\delta\text{ISW}}{\text{ISW}} = \sum_{\ell, z} \frac{C_{gT}(\ell, z + \Delta z)/C_{gT}(\ell, z)}{\Delta C_{gT}^2(\ell, z)/C_{gT}^2(\ell, z)} / \sum_{\ell, z} \frac{1}{\Delta C_{gT}^2(\ell, z)/C_{gT}^2(\ell, z)}, \quad (26)$$

which, for small  $\Delta z$ , yields

$$\frac{|\delta\text{ISW}|}{\text{ISW}} \simeq \frac{1}{2} \left| \sum_{\ell, z} \frac{\Delta z \cdot \partial C_{gT}^2(\ell, z)/\partial z}{\Delta C_{gT}^2(\ell, z)} \right| / \sum_{\ell, z} \frac{C_{gT}^2(\ell, z)}{\Delta C_{gT}^2(\ell, z)} \lesssim 3 \Delta z, \quad (27)$$

where we used Eqs. (11-13) to estimate the numerical value of the above expression. Since the optimum signal-to-noise for an ISW detection is  $\sim 7$ , the redshift systematic errors may not dominate the errors if

$$\Delta z_{sys} \lesssim \frac{1}{3 \times 7} \simeq 0.05. \quad (28)$$

## VI. WHAT DOES ISW TELL US ABOUT COSMOLOGY?

Let us study the optimum constraints that an ISW cross-correlation detection can give us about cosmology. For a nominal concordance cosmology  $\mathcal{C}_0$ , the expected significance level for ruling out the cosmology  $\mathcal{C}$ ,  $\chi$ , is given by

$$\chi^2 = \sum_{\ell, z} \frac{[C_{gT}(\ell, z; \mathcal{C}) - C_{gT}(\ell, z; \mathcal{C}_0)]^2}{\Delta C_{gT}^2(\ell, z; \mathcal{C}_0)}, \quad (29)$$

where  $C_{gT}$  and  $\Delta C_{gT}$  are defined in Eqs. (11-13). Note that the bias factor,  $b_g$ , is cancelled from the numerator

and the denominator, and the optimum significance level only depends on the fluctuations in matter density and gravitational potential.

Fig. (6) shows the optimum constraints that an ISW detection may yield on some of the properties of dark energy, i.e. its density, equation of state, and speed of sound [22]. While such constraints are already comparable to the current bounds on these parameters [9, 21, 23], future observations of CMB and large scale structure [24] will significantly improve these bounds. However, ISW constraints could still be used to test possible systematics that may affect the accuracy of future measurements.

It has been claimed [25] that the cross-correlation observations could be used to break the degeneracies in the so-called doomsday cosmological scenarios, which involve a varying equation of state. However, given the cosmic variance limited measurements of the ISW effect (Eq. 29), it does not seem that such constraints can significantly improve the expected combined constraints from the upcoming Planck and SNAP satellite experiments [26, 27]

A more intriguing application of an ISW detection is the possibility of testing our theories of matter/gravity on large scales [28]. While the consistency of the power spectrum of 2dF and SDSS galaxy surveys [29] with the  $\Lambda$ CDM power spectrum confirms the consistency of the  $\Lambda$ CDM concordance cosmology at scales of  $k \gtrsim 0.1 h \text{ Mpc}^{-1}$ , Fig.(7) shows that an ISW detection can do the same at scales of  $k \sim 0.003 - 0.03 h \text{ Mpc}^{-1}$ . Therefore, current [6, 7] and future observations of an ISW effect may confirm the consistency of our cosmological theories at the largest physical scales that they have ever been tested. While the cross-correlation statistics are almost free of systematic bias, the auto-correlation is often dominated by survey systematics on such scales.

## VII. CONCLUSIONS

In this paper, we study different aspects of the correlation between a galaxy survey and CMB sky, due to the ISW effect in a flat universe. The main source of noise is contamination by the primary CMB anisotropies. We see that, given this noise, most of the signal comes from  $\ell \sim 20$ , and  $z \sim 0.4$  with negligible contribution from  $\ell > 100$  and  $z > 1.5$ .

While the maximum significance level for an ISW detection is  $\sim 7.5\sigma$  for a concordance  $\Lambda$ CDM cosmology, an all-sky survey with about 10 million galaxies within  $0 < z < 1$  should yield an almost perfect ISW detection, at the  $\sim 5\sigma$  level.

We show that, in order to achieve a cosmic-variance limited ISW detection, the systematic anisotropies of the galaxy survey must be below 0.1%, on the scale of  $\sim 10$  degrees on the sky. Within this level of systematics, and given the current level of Galactic contamination in WMAP CMB maps ( $\sim \mu K$ ), there should be a negligible over/underestimate of the ISW signal due to the system-

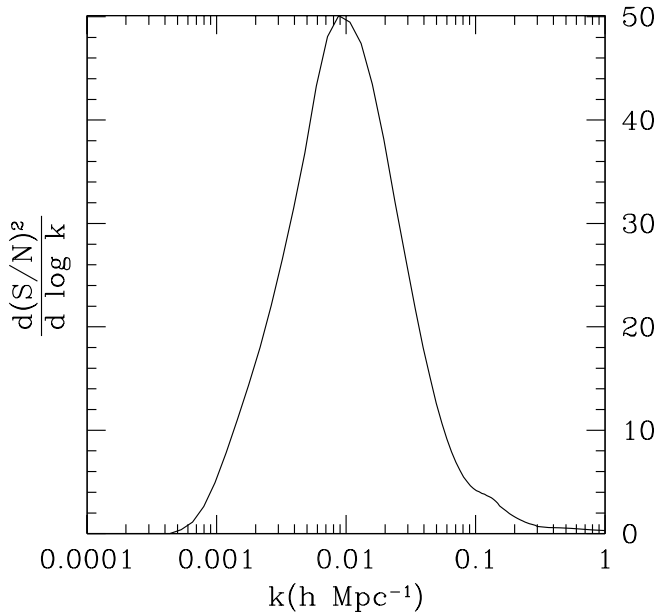


FIG. 7: The distribution of  $(S/N)^2$  of an ISW detection in  $k$ -space.

atic correlations of CMB and galaxy maps. We also argue that, while the random uncertainties in redshifts cannot

significantly reduce the significance of an ISW detection, the systematic errors in redshift estimates need be less than 0.05, in order to achieve a cosmic-variance limited measurement.

It turns out that, due to the large noise induced by the primary anisotropies, the optimum constraints on the properties of dark energy from an ISW detection, are already comparable to the current accuracies, and will be outdone by future observations. However, the simplicity of the linear physics involved in the ISW effect, and the fact that the cross-correlation statistics are not biased by the systematics of CMB or galaxy surveys, makes ISW detection a useful indicator of possible systematics in more accurate methods.

Finally, we point out that the detection of the ISW effect provides a unique test of our concordance cosmological model on the largest physical scales that it has ever been tested.

#### Acknowledgments

The author wishes to thank Steve Boughn, Yeong-Shang Loh, David Spergel, and Michael Strauss for illuminating discussions and useful comments. This work was originated as response to a question asked by Yeong-Shang Loh, and the author is grateful to him for asking that question.

- 
- [1] G. F. Smoot *et al.*, *Astrophys. J. Lett.* **396**, 1 (1992).  
 [2] C. L. Bennett *et al.*, *Astrophys. J. Supp.* **148**, 1 (2003).  
 [3] See for example: W. Hu, and S. Dodelson, *Ann. Rev. Astron. Astrophys.* **40**, 171 (2002).  
 [4] R. G. Crittenden, and N. Turok, *Phys. Rev. Lett.* **76**, 575 (1996).  
 [5] H. Peiris, and D. N. Spergel, *Astrophys. J.* **540**, 605 (2000); A. Cooray, *Phys. Rev. D* **65**, 103510 (2002).  
 [6] S. P. Boughn, and R. G. Crittenden, *Nature (London)* **427**, 45 (2004); M. R. Nolta *et al.*, *Astrophys. J.* **608**, 10 (2004); P. Fosalba, E. Gaztañaga, and F. Castander, *Astrophys. J. Lett.* **597**, 89 (2003); P. Fosalba and E. Gaztanaga, *Mon. Not. Roy. Astron. Soc.* **350**, L37 (2004); R. Scranton *et al.* (SDSS Collaboration), *astro-ph/0307335*.  
 [7] N. Afshordi, Y. S. Loh and M. A. Strauss, *Phys. Rev. D* **69**, 083524 (2004).  
 [8] R. K. Sachs, and A. M. Wolfe, *Astrophys. J.* **147**, 73 (1967).  
 [9] D. N. Spergel *et al.*, *Astrophys. J. Supp.* **148**, 175 (2003).  
 [10] P. J. E. Peebles, and B. Ratra, *Rev. Mod. Phys.* **75**, 599, (2003).  
 [11] For example, see V.F. Mukhanov, H. A. Feldman, and R. H. Brandenberger, *Phys. Rep.* **215**, 203 (1992).  
 [12] M. Kesden, M. Kamionkowski, and A. Cooray, *Phys. Rev. Lett.* **91**, 221302 (2003).  
 [13] G. Hinshaw *et al.*, *Astrophys. J. Supp.* **148**, 135 (2003).  
 [14] D. G. York *et al.* [SDSS Collaboration], *Astron. J.* **120**, 1579 (2000).  
 [15] <http://www.lsst.org/>; <http://pan-starrs.ifa.hawaii.edu/>.  
 [16] C. Bennett *et al.*, *Astrophys. J. Suppl.* **148** (2003) 97.  
 [17] M. R. Blanton *et al.*, *Astrophys. J.* **592**, 819 (2003).  
 [18] K. Abazajian *et al.* [SDSS Collaboration], *Astron. J.* **126**, 2081 (2003).  
 [19] D. J. Schlegel, D. P. Finkbeiner and M. Davis, *Astrophys. J.* **500** (1998) 525.  
 [20] P. Schechter, *Astrophys. J.* **203**, 297 (1976).  
 [21] M. Tegmark *et al.* [SDSS Collaboration], *Phys. Rev. D* **69**, 103501 (2004).  
 [22] For details of the cosmological perturbation theory with dark energy, see: J. Erickson *et al.*, *Phys. Rev. Lett.* **88**, 121301 (2002).  
 [23] R. Bean and O. Dore, *Phys. Rev. D* **69**, 083503 (2004).  
 [24] For example see W. Hu, and Z. Haiman, *Phys. Rev. D* **68**, 063004 (2003); Y. Song, and L. Knox, *astro-ph/0312175*.  
 [25] J. Garriga, L. Pogosian and T. Vachaspati, *Phys. Rev. D* **69**, 063511 (2004).  
 [26] J. Kratochvil, Private Communication.  
 [27] J. Kratochvil, A. Linde, E. V. Linder and M. Shmakova, *JCAP* **0407**, 001 (2004).  
 [28] A. Lue, R. Scoccimarro and G. Starkman, *Phys. Rev. D* **69**, 044005 (2004).  
 [29] M. Tegmark, A.J.S. Hamilton, and Y. Xu, *Mon. Not. R. Astron. Soc.* **335**, 887 (2002); M. Tegmark *et al.* [SDSS Collaboration], *Astrophys. J.* **606**, 702 (2004).  
 [30] This statement is strictly valid only for wavelengths much larger than the Hubble radius, or if the speed of sound vanishes.  
 [31] The error in the Limber approximation, in the form ex-



pressed here, is about 10% at  $\ell = 2$  and drops as  $\ell^{-2}$ .

- [32] If the survey does not cover the whole sky, the nearby multipoles in the harmonic space will not be independent. However, if we bin a large number of multipoles together,

we can use the increased standard deviation of Eq. (9) for each multipole and treat them as independent to estimate the error of each multipole bin.